

In Situ, Vibrationally Resonant Sum Frequency Spectroscopy Study of the Self-Assembly of Dioctadecyl Disulfide on Gold

Clayton S.-C. Yang, Lee J. Richter,* John C. Stephenson, and Kimberly A. Briggman

National Institute of Standards and Technology, 100 Bureau Drive,
Gaithersburg, Maryland 20899-8372

Received March 26, 2002. In Final Form: May 24, 2002

We report the results of an in situ, vibrationally resonant sum frequency generation (SFG) spectroscopy study of the assembly of perdeuterated dioctadecyl disulfide on gold substrates from ethanol solutions under laminar flow conditions. The coverage evolution of the SFG spectra can be well described by the coexistence of two distinct phases: a low-coverage, disordered phase and the full-coverage crystalline phase. The structure of the adsorbed thiolate fragments in the low-coverage phase is disordered but upright (as opposed to lying completely in the surface plane), characterized by significant gauche defects in the backbone but a near-normal orientation for the terminal methyl group. The crystalline phase is marked by an erect all-trans configuration of the alkane chain. The kinetics of the evolution of these two phases can be quantitatively described by a simple model, consistent with phase coexistence above a critical density of the disordered phase.

I. Introduction

Self-assembled monolayers (SAMs) are ordered molecular assemblies formed spontaneously by the adsorption of a molecule with a certain affinity of its headgroup to the substrate. Among SAMs, the assembly of organosulfur compounds, especially thiols (R–S–H) and disulfides (R–S–S–R), on coinage metals has received considerable attention.^{1–4} These SAMs are excellent model systems for studies of monolayer structure,^{5–7} adhesion,⁸ and interfacial reactions^{9–11} and have novel applications as biosensors^{12,13} and corrosion inhibitors.¹⁴ The adsorption of alkanethiol molecules on Au from both solution and the gas phase has been extensively studied and recently reviewed.^{15,16} There has been much less attention paid to the adsorption of dialkyl disulfides.^{17–20} It is well established that the disulfides and thiols result in indistin-

guishable monolayers, composed of erect gold thiolate (RS⁻) species.^{17,18} However, there have been very few studies of the evolution of the surface species with coverage.

Surprisingly, even for the extensively studied alkanethiolates, there have been few vibrational spectroscopy studies of the assembly that probe the full coverage range and no in situ kinetic vibrational spectroscopy studies. Early ex situ infrared reflection–absorption spectroscopy (IRAS) and vibrationally resonant sum frequency generation (SFG) studies focused on the structure of the completed films.^{21–23} More recently, ex situ studies have been performed on partial monolayers removed from solution and rinsed to remove loosely attached adsorbate molecules.^{24–26} However, changes of the film coverage and structure can occur in an ex situ measurement.²⁷ Therefore, in situ studies under actual deposition conditions in real time are preferable.

Second-order nonlinear optical techniques are particularly well suited for probing chemical reactions at buried interfaces due to their high surface selectivity, submonolayer sensitivity, and excellent spatial, spectral, and temporal resolution.²⁸ Vibrationally resonant SFG, in which a vibrationally resonant IR photon is mixed with a visible photon in a second-order process, has the additional advantage of being able to probe the vibrational spectra of buried interfaces and thus provide insight into alkane chain order and orientation.²⁹ In this paper, we report an in situ SFG study of the assembly of SAMs from

* Corresponding author. E-mail: lee.richter@nist.gov.

(1) Nuzzo, R. G.; Fusco, F. A.; Allara, D. L. *J. Am. Chem. Soc.* **1987**, *109*, 2358.

(2) Bain, C. D.; Troughton, E. B.; Tao, Y.-T.; Evall, J.; Whitesides, G. M.; Nuzzo, R. G. *J. Am. Chem. Soc.* **1989**, *111*, 321.

(3) Dubois, L. H.; Nuzzo, R. G. *Annu. Rev. Phys. Chem.* **1992**, *43*, 437.

(4) Ulman, A. *An Introduction to Ultrathin Organic Films*; Academic Press: Boston, 1991.

(5) Bain, C. D.; Whitesides, G. M. *J. Am. Chem. Soc.* **1988**, *110*, 3665.

(6) Chidsey, C. E. D.; Liu, G.-Y.; Rowntree, P.; Scoles, G. *J. Chem. Phys.* **1989**, *91*, 4421.

(7) Bareman, J. P.; Klein, M. L. *J. Phys. Chem.* **1990**, *94*, 5202.

(8) Lopez, G. P.; Albers, M. W.; Schreiber, S. L.; Carroll, R.; Peralta, E.; Whitesides, G. M. *J. Am. Chem. Soc.* **1993**, *115*, 5877.

(9) Xu, C.; Sun, L.; Kepley, L. J.; Crooks, R. M.; Ricco, A. J. *Anal. Chem.* **1993**, *65*, 2102.

(10) Duevel, R. V.; Corn, R. M. *Anal. Chem.* **1992**, *64*, 337.

(11) Weisshaar, D. E.; Lamp, B. D.; Porter, M. D. *J. Am. Chem. Soc.* **1992**, *114*, 5860.

(12) Thoden van Velzen, E. U.; Engberson, J. F. J.; de Lange, P. J.; Mahy, J. W. G.; Reindhoudt, D. N. *J. Am. Chem. Soc.* **1995**, *117*, 6853.

(13) Motesharei, K.; Myles, D. C. *J. Am. Chem. Soc.* **1998**, *120*, 7328.

(14) Laibinis, P. E.; Whitesides, G. M. *J. Am. Chem. Soc.* **1992**, *114*, 9022.

(15) Ulman, A. *Chem. Rev.* **1996**, *96*, 1533.

(16) Schreiber, F. *Prog. Surf. Sci.* **2000**, *65*, 151.

(17) Bain, C. D.; Biebuyck, H. A.; Whitesides, G. M. *Langmuir* **1989**, *5*, 723.

(18) Biebuyck, H. A.; Bain, C. D.; Whitesides, G. M. *Langmuir* **1994**, *10*, 1825.

(19) Jung, C.; Dannenberger, O.; Xu, Y.; Buck, M.; Grunze, M. *Langmuir* **1998**, *14*, 1103.

(20) Shon, Y.-S.; Lee, R. T. *J. Phys. Chem. B* **2000**, *104*, 8182.

(21) Nuzzo, R. G.; Dubois, L. H.; Allara, D. L. *J. Am. Chem. Soc.* **1990**, *112*, 558.

(22) Parikh, A. N.; Allara, D. L. *J. Chem. Phys.* **1992**, *96*, 927.

(23) Terrill, R. H.; Troy, T. A.; Bohn, P. W. *Langmuir* **1998**, *14*, 845.

(24) Truong, K. D.; Rowntree, P. A. *Prog. Surf. Sci.* **1995**, *50*, 207.

(25) Himmelhaus, M.; Eisert, F.; Buck, M.; Grunze, M. *J. Phys. Chem. B* **2000**, *104*, 576.

(26) Bensebaa, F.; Voicu, R.; Huron, L.; Ellis, T. H.; Kruus, E. *Langmuir* **1997**, *13*, 5335.

(27) Schwartz, D. K. *Annu. Rev. Phys. Chem.* **2001**, *52*, 107.

(28) Shen, Y. R. *Surf. Sci.* **1994**, *300*, 551.

(29) Bain, C. D. *J. Chem. Soc., Faraday Trans.* **1995**, *91*, 1281.

dioctadecyl disulfide on gold from ethanol solutions. The kinetics and mechanisms of film formation are found to be similar to those of the related, well-studied thiol molecules on gold. The uptake of surface thiolate is found to follow Langmuir kinetics, and the conformation and ordering of the alkane chain are strongly dependent on coverage. A simple model, in which the surface is covered with two molecular phases (disordered and crystalline) in coexistence, is found to describe the evolution of molecular structure with surface density.

II. Experiment

Perdeuterated octadecanethiol (dODT) was synthesized and generously provided by Professor David Allara, Penn State University. Perdeuterated octadecane disulfide (dODDS) was synthesized and purified by Dr. David Vanderah, NIST.³⁰ The purity of both materials was confirmed to be >95% by thin film chromatography. Absolute (200 proof) ethanol (EtOH) from the Warner-Graham Co., Cockeysville, MD, was used as received.³¹ The Au substrates were nominally 200 nm thick, vapor-deposited films on a ≈ 1 nm Cr adhesion layer on glass substrates. The Au films were cleaned by a 15 min activated oxygen treatment in an UV-ozone cleaner, followed by exposure to flowing EtOH for 10 min to reduce the resultant thin gold oxide layer.³² The oxygen-cleaned surfaces were hydrophilic (water contact angle of less than 3°) and showed negligible vibrationally resonant SFG signatures in the CD and CH regions prior to exposure to EtOH.

The experimental approach used in our broadband SFG measurements has been described in detail elsewhere.³³ The SFG apparatus consists of a commercial, tunable, 50 fs Ti:sapphire laser system, which is used to pump an optical parametric amplifier after pulse amplification to generate tunable broadbandwidth (250 cm^{-1} full width at half-maximum (fwhm)) signal (1100–1600 nm) and idler (1600–2600 nm) pulses. Difference frequency generation between these pulses in a 1 mm AgGaS₂ crystal produces broadbandwidth (300 cm^{-1} fwhm) IR pulses tunable from 2.5 to 12 μm . The visible probe beam was a bandwidth-narrowed (4 cm^{-1} fwhm) 810 nm beam derived from the amplified Ti:sapphire laser pulse. The resolution of the SFG spectra is determined by the bandwidth of this visible probe. Note that the laser setup used for this study is different from that of ref 33; it produces pulses of shorter duration and broader spectral width. Also, in contrast to ref 33, to achieve the bandwidth-narrowed visible probe, a partial reflecting mirror sent the entire spectrum of the uncompressed amplified 810 nm pulses to the bandwidth-limiting Czerny–Turner monochromator. The generated SF light centered at 680 nm was collected and dispersed in a spectrometer. A scientific grade CCD detector was used to detect the entire spectrum of the SF light in parallel. Experiments reported herein used broad-bandwidth IR pulses in the frequency range of 1900–2300 cm^{-1} . Pairs of half-wave plates and polarizers in the optical pathway were used to control the polarization of the 810 nm and SFG beams. All SFG spectra reported were taken with a ppp polarization combination, in which the IR, visible, and detected SFG photons were polarized in the plane of incidence.

The in situ sample cell was a FCS2 microscopy chamber from Biopetechs (Butler, PA).³¹ A 25 μm Teflon³¹ spacer was sandwiched between a 1 mm calcium fluoride entrance window and the Au substrate inside the chamber. The Au-coated substrate was a microaqueduct slide with two T-shaped grooves ≈ 12 mm long that allow laminar flow in a ≈ 20 mm long channel across the sample. The nominal volume of the flow cell was 6 μL . A peristaltic pump was used to pull solution through the cell at a maximum

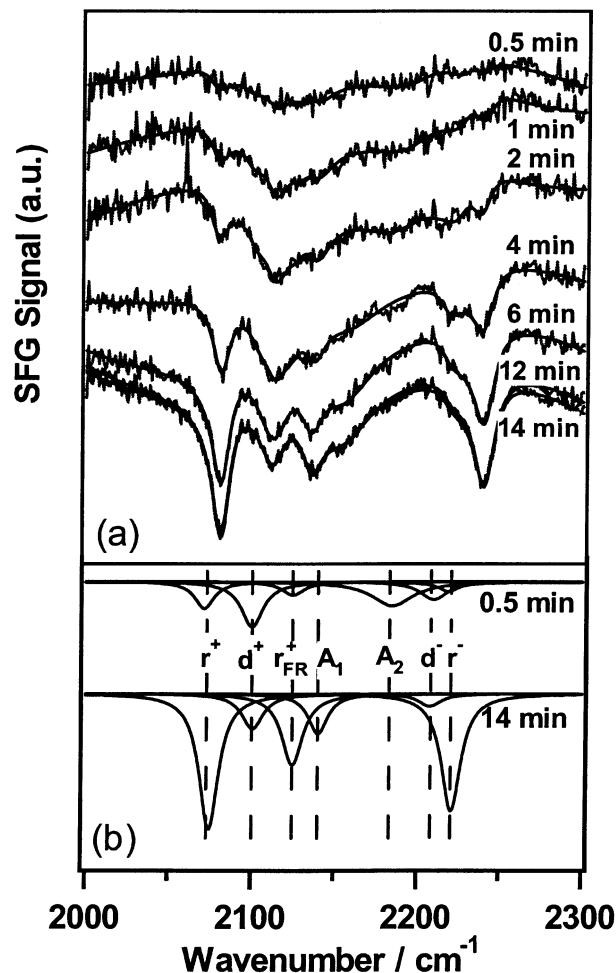


Figure 1. (a) The time evolution of the SFG spectra of dODDS on gold; (b) the imaginary part of the Lorentzian components of an early-time spectrum (0.5 min) and a late-time spectrum (14 min). For mode assignments, see Table 1.

flow rate of about 1.1 mL/min. The surface was kept in contact with flowing solution throughout the collection of SFG spectra. A 25 mL glass jar was used as a sample reservoir, and stainless steel tubing (~ 0.6 mm i.d.) connected the reservoir and the pump to the sample cell. The IR and visible beams were focused to a beam waist of ~ 100 μm and were coincident on the calcium fluoride window at 67° and 45° with respect to the surface normal. Due to refraction, the incident angles were nominally 43° and 32° at the solution/Au interface. For the ex situ spectra, the incident angles were changed to allow better comparison to the in situ spectra and were $\approx 45^\circ$ and 23° , respectively, at the air/Au interface. The IR pulse energy was 3.5 μJ , and the visible pulse energy was 1.8 μJ .

III. Results

The time evolution of SFG spectra following the adsorption of dODDS from an EtOH solution on gold is shown in Figure 1. IR absorption by the solution prohibits the study of protonated ODT in EtOH even though the solution layer between the window and the sample is 25

(30) The perdeuterated dioctadecyl disulfide ($\text{C}_{36}\text{D}_{74}\text{S}_2$, dODDS) was obtained as a minor component of the preparation of perdeuterated octadecanethiol from perdeuterated octadecanol ($\text{C}_{18}\text{D}_{37}\text{OH}$) [Cambridge Isotope Laboratories, Andover, MA]. Perdeuterated octadecanol was first converted to the corresponding bromide [CBr_4 and $(\text{C}_6\text{H}_5)_3\text{P}/\text{THF}$, 1 h, room temperature, 100%]. The brominated compound was then reacted with $\text{CH}_3\text{COSNa}/\text{MeOH}$ and refluxed for 8 h. This yielded the perdeuterated octadecanethiol as the major product (32%) and the disulfide as a minor product (25%). The disulfide was purified (single spot by thin layer chromatography) by column chromatography [silica gel, $R_f = 0.72$ (hexane), EI ($M^+ = 646$)].

(31) We identify certain commercial equipment, instruments, or materials in this article to adequately specify the experimental procedure. In no case does such identification imply recommendation or endorsement by the National Institute of Standards and Technology, nor does it imply that the materials or equipment identified are necessarily the best available for the purpose.

(32) Woodward, J. T.; Walker, M. L.; Meuse, C. W.; Vanderah, D. J.; Poirier, G. E.; Plant, A. L. *Langmuir* **2000**, *16*, 5347 and references therein.

(33) Richter, L. J.; Petralli-Mallow, T. P.; Stephenson, J. C. *Opt. Lett.* **1998**, *23*, 1594.

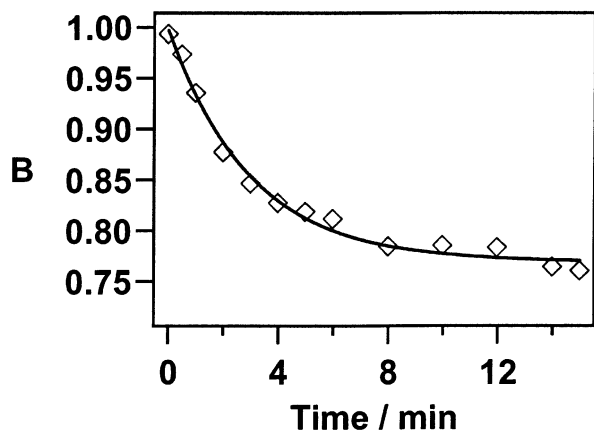


Figure 2. The time dependence of the nonresonant background, B , for dODDS uptake on Au. The solid line represents the fit to the Langmuir kinetics model.

μm . Attempts to study protonated ODT in perdeuterated methanol failed due to surface-active hydrocarbon contaminants. After the flow starts, series SFG spectra are taken every 30 s. The spectra are referenced to the spectrum at $t = -1$ min, prior to the introduction of disulfide. For ease of comparison with linear vibrational spectroscopies, the x -axis is set to the incident IR wavenumber. The flow rate was 1.1 mL/min, and the concentration of dODDS was 0.24 $\mu\text{mol/L}$. The SFG spectrum can be modeled by the form

$$I_{\text{ppp}} = |B + \sum_i \frac{A_i e^{i\phi_i}}{\nu_{\text{IR}} - \nu_i + i\Gamma_i}|^2 \quad (1)$$

where B corresponds to the nonresonant signal and the sum is over the vibrationally resonant contributions from the adsorbate molecules.³⁴ The factor ϕ_i accounts for phase differences between the contributions to the spectra. A_i , ν_i , and Γ_i correspond to the amplitude, frequency, and spectral width of each resonant feature, respectively. Solid lines shown in Figure 1 are fits of the spectra to this form, with seven resonant features between 1900 and 2300 cm^{-1} .

The Au interface has a strong hyperpolarizability³⁵ that completely dominates B . The development of a thiolate bond on the Au surface reduces the Au hyperpolarizability and consequently the nonresonant background, B . This change of Au nonresonant signal by thiolate bond formation has been used to study the adsorption kinetics in previous in situ second harmonic generation (SHG)^{36,37} and ex situ SFG²⁵ studies. The time dependence of B is shown in Figure 2. In previous studies of related thiol systems,^{25,36–41} it has been found that a Langmuir model adequately represents the adsorption kinetics. In a Langmuir model, the rate of adsorption is assumed to be proportional to the free space on the surface and the flux of attempting species (which is proportional to the disulfide concentration C in solution). That is, $d\theta/dt = 2kC(1 - \theta)$,

where the factor of 2 accounts for the two surface thiolate molecules formed per adsorbing disulfide molecule, θ is the normalized surface thiolate coverage ($\equiv 1$ at saturation), and k is the effective rate constant for thiolate bond formation. This leads to the integrated expression $\theta = 1 - \exp(-2kCt) = 1 - \exp(-t/\tau)$. The solid line in Figure 2 represents a least-squares fit to this functional form and the assumption that B varies linearly with coverage: $B = B_0 - R\theta$. The rate constant k derived from the fitted value of τ and the bulk disulfide concentration C is $1.0 \times 10^4 \text{ L mol}^{-1} \text{ s}^{-1}$. A similar rate constant of $k = 1.2 \times 10^4 \text{ L mol}^{-1} \text{ s}^{-1}$ was determined in preliminary measurements on the adsorption of dODT [in this case with the convention $d\theta/dt = kC(1 - \theta)$].

Deviations from the time dependence, $\theta = 1 - \exp(-t/\tau)$, implied by the Langmuir model can arise from two principal causes: the rate law deviates from a $(1 - \theta)$ form or the concentration of solute at the surface $C[0]$ becomes time dependent due to transport effects. Recently, Jung and Campbell³⁸ carefully studied the adsorption of alkanethiol molecules in a stop flow experiment and accounted for the transport effects on $C[0]$ by solving the drift-diffusion equations for $C[0]$ self-consistently with the observed rate of adsorption. A strict $(1 - \theta)$ scaling was found for the initial $\sim 80\%$ of thiol uptake. In our channel flow configuration, $C[0]$ can be determined from solutions to the convection-diffusion equations with the assumption of laminar flow. The initial adsorption flux ($2kC\sigma_{\text{sat}}$, $\sigma_{\text{sat}} = 4.5 \times 10^{14} \text{ cm}^{-2}$, the saturation coverage¹⁶) is balanced by a diffusive flux ($2D\partial C[0]/\partial z$) where z is the normal to the surface. $\partial C[0]/\partial z$ is determined by the characteristic length⁴²

$$\delta = \sqrt[3]{\frac{DLh}{3V_a}} \quad (2)$$

where D is the diffusion coefficient (estimated⁴³ as $4.5 \times 10^{-6} \text{ cm}^2 \text{ s}^{-1}$), L is the length of the channel upstream of the measurement position (1 cm), h is the channel height (0.0025 cm), and V_a is the average stream velocity (6 cm s^{-1} for 1.1 mL min^{-1} flow). The estimated diffusion-limited flux of $2DC/\delta = 1.5 \times 10^{12} \text{ molecules cm}^{-2} \text{ s}^{-1}$ is comparable to the adsorption rate deduced from the measured time constant τ for the reduction in the nonresonant background, $\sigma_{\text{sat}}/\tau = 2.1 \times 10^{12} \text{ molecules cm}^{-2} \text{ s}^{-1}$, suggesting that the uptake is close to transport limited. At flow rates of 0.34 mL min^{-1} and less, an incubation time became evident in the data. This is because the upstream portions of the channel completely deplete the solute from the stream of solvent. At a flow of 0.68 mL min^{-1} , k derived from the fitted τ is $1.2 \times 10^4 \text{ L mol}^{-1} \text{ s}^{-1}$. At flow rates greater than 1.1 mL min^{-1} , the cell leaked and prevented measurement.

We have performed numerical finite difference calculations using the physical parameters of our system to investigate the behavior when the kinetics is close to diffusion limited, that is, when $DC/\delta \sim \kappa C\sigma_{\text{sat}}$ where κ is the true surface reaction rate. The onset of diffusion-limited behavior is clearly reflected in marked deviations from the Langmuir form for the time evolution of surface coverage θ : the uptake of thiolate becomes linear in time. Note this is different from the case of stop flow: for channel

(34) Stanners, C. D.; Du, Q.; Chin, R. P.; Cremer, P.; Somorjai, G. A.; Shen, Y. R. *Chem. Phys. Lett.* **1995**, *232*, 407.

(35) Koos, D. A.; Richmond, G. L. *J. Phys. Chem.* **1992**, *96*, 3770.

(36) Dannenberger, O.; Buck, M.; Grunze, M. *J. Phys. Chem. B* **1999**, *103*, 2202.

(37) Dannenberger, O.; Wolff, J. J.; Buck, M. *Langmuir* **1998**, *14*, 4679.

(38) Jung, L. S.; Campbell, C. T. *J. Phys. Chem. B* **2000**, *104*, 11168.

(39) Peterlinz, K. A.; Georgiadis, R. *Langmuir* **1996**, *12*, 4731.

(40) Schessler, H. M.; Karpovich, D. S.; Blanchard, G. J. *J. Am. Chem. Soc.* **1996**, *118*, 9645.

(41) Xu, S.; Sylvain, J. N.; Cruchon-Dupeyrat, S. J. N.; Garno, J. C.; Liu, G.-Y.; Jennings, G. K.; Yong, T.-H.; Laibinis, P. E. *J. Chem. Phys.* **1998**, *108*, 5002.

(42) Levich, V. G. *Physicochemical Hydrodynamics*, Prentice Hall: Englewood Cliffs, NJ, 1962.

(43) D was estimated based on the value $5.7 \times 10^{-6} \text{ cm}^2 \text{ s}^{-1}$ for octadecanethiol in ref 38, the Stokes–Einstein relationship, and the assumption that the hydrodynamic radius of the disulfide is $2^{1/3}$ that of the thiol.

flow the concentration diffusion length is fixed by the flow velocity and independent of C , while for stop flow the concentration diffusion length varies with time and C . The excellent agreement between the Langmuir model and our observed data implies that we are not significantly influenced by diffusion effects; that is, the flux of reacting molecules at the surface must be almost constant over the course of the experiment, within a factor of ~ 2 of that for the non-diffusion-limited case. This implies that we have overestimated the diffusion length δ , most likely due to an underestimation of the true channel height at the measurement point. The values of k deduced by assuming the bulk reactant concentration available at the surface might be in error (too small) by a factor of ~ 2 . Therefore, we feel that although we may slightly underestimate k by identifying $1/\tau = 2kC$, assuming the bulk value of C , the interpretation of these experiments is otherwise unaffected.

The resonant features between 1900 and 2300 cm^{-1} can be generally attributed to the C–D stretching vibrational modes of CD_2 and CD_3 groups based on the spectra of perdeuterated polyethylene⁴⁴ and short-chain deuterated alkanes⁴⁵ as shown in Table 1. The weak features at 2145 and 2167 cm^{-1} present in early-time spectra are assigned to the symmetric CD_2 stretch (d^+) in Fermi resonance, similar to features in the IR spectra of protonated ODT.²² Starting from the structureless spectra at time zero, distinct vibrational features evolve and change with progressing adsorption time. Up to 3 min after the flow starts, a strong and broad d^+ feature at 2103 cm^{-1} dominates the spectra. For $t > 3$ min, this d^+ spectral feature sharpens and methyl features appear at 2130 cm^{-1} (symmetric stretch r^+) and 2220 cm^{-1} (asymmetric stretch r^-) while the methylene features fade.

Figure 3 shows a comparison of the ex situ SFG spectrum of a film formed in the flow cell ($0.48 \times 10^{-6} \text{ mol L}^{-1}$, flow rate 0.68 mL min^{-1} for 14 min) to the spectrum of a film formed by static soaking the substrate in a large vessel ($0.48 \times 10^{-6} \text{ mol L}^{-1}$ solution for over 24 h). There is no difference in the level of the nonresonant background, to within an 8% reproducibility of the measurement. At 24 h, there are minor changes in the spectra: the CD_3 modes slightly intensify at the expense of the CD_2 modes, as reported in Table 2. Also shown in Figure 3 is an ex situ SFG spectrum formed by soaking in a $3 \times 10^{-6} \text{ mol/L}$ solution of dODT for over 140 h. All three spectra are referenced to the spectrum of the cleaned gold taken prior to the introduction of disulfide. There are no significant differences observed by SFG in the final films formed from DODDS and dODT.

IV. Discussion

We begin with a review of the behavior of the more extensively studied adsorption of alkanethiol molecules. In the case of adsorption from the vapor phase, the process proceeds via the formation of distinct phases of surface species.⁴⁶ At low exposures, an ordered striped phase, attributed to extended molecules lying in the surface plane, is formed with a near-unity sticking coefficient.⁴⁷ With increasing exposure, an intermediate (IM), disordered

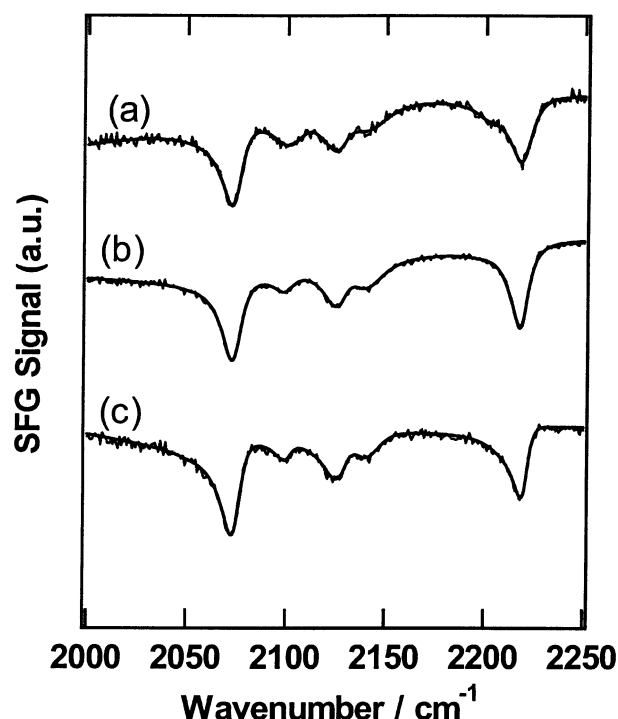


Figure 3. Ex situ ppp SFG spectra: (a) dODDS film formed by exposure to 14 min of 0.68 mL/min flowing solution at a concentration of $0.48 \mu\text{mol L}^{-1}$; (b) dODDS film formed by soaking in a $0.48 \mu\text{mol L}^{-1}$ solution for 24 h; (c) dODT film formed by soaking in a $3 \mu\text{mol L}^{-1}$ solution for 140 h. These spectra have been offset for clarity.

Table 1. Assignment of C–D Stretching Modes

description	symbol	wavenumber (cm^{-1})
1. CD_3 , symmetric	r^+	2073
2. CD_2 , symmetric	d^+	2103
3. CD_3 , symmetric Fermi resonance	r^+_{FR}	2130
4. CD_2 , symmetric Fermi resonance	A_1	2145
5. CD_2 , symmetric Fermi resonance	A_2	2167
6. CD_2 , antisymmetric	d^-	2200
7. CD_3 , antisymmetric	r^-	2220

Table 2. Fit Parameters for the SFG Spectra of Films Formed from DODDS in Figure 3^a

	14 min	24 h
1. A_{r^+}	0.66 ± 0.05	0.68 ± 0.04
2. A_{d^+}	0.22 ± 0.04	0.11 ± 0.01
3. A_{r^-}	0.62 ± 0.11	0.70 ± 0.03
4. A_{r^+}/A_{d^+}	3.00 ± 0.22	6.18 ± 0.36
5. A_{r^-}/A_{r^+}	0.94 ± 0.16	1.02 ± 0.04
6. Γ_{r^+}	5.9 ± 0.12	5.9 ± 0.03
7. B	0.75 ± 0.01	0.71 ± 0.01

^a Errors are determined from the fit of eq 1 to the data.

phase is formed with a lower sticking coefficient.⁴⁶ The molecular structure in the intermediate phase is not known. Finally, at high exposures, a crystalline phase with a $\sqrt{3} \times \sqrt{3}$ lattice and a $c(4 \times 2)$ superstructure nucleates in the IM phase and grows as islands. The sticking coefficient for molecules incorporated into the crystalline phase is ≈ 500 times lower than that for incorporation into the stripe phase.⁴⁶ In the crystalline phase, the molecules are erect, in a nearly all-trans configuration, tilted by $\approx 30^\circ$ from the surface normal.¹⁶ The overall kinetics of adsorption can be described by two independent Langmuir terms.⁴⁶

In the case of adsorption of alkanethiol molecules from solution, there is considerable variability in the reported

(44) Tasumi, M.; Shimanouchi, T.; Tanaka, H.; Ikeda, S. *J. Polym. Sci.* **1964**, *A2*, 1607.

(45) Schachtschneider, J. H.; Snyder, R. G. *Spectrochim. Acta* **1963**, *19*, 117.

(46) Schreiber, F.; Eberhardt, A.; Leung, T. Y. B.; Schwartz, P.; Wetterer, S. M.; Lavrich, D. J.; Berman, L.; Fenter, P.; Eisenberger, P.; Scoles, G. *Phys. Rev. B* **1998**, *57*, 12476.

(47) Schwartz, P.; Schreiber, F.; Eisenberger, P.; Scoles, G. *Surf. Sci.* **1999**, *423*, 208.

kinetics. This can be attributed, in part, to the sensitivity of the adsorption to the cleanliness and texture of the substrate, the purity of the solution, and the specific nature of the solvent.³⁹ However, a general consensus has developed for the most commonly used ethanol and heptane solvents. Under conditions of flow, or stop flow when the solute diffusion is properly accounted for, the thiol molecules exhibit single Langmuir adsorption kinetics for at least the first $\approx 80\%$ of the uptake of the coverage. The concentration-normalized rate constant for adsorption from solution is typically 10^6 times smaller than the near-unity sticking coefficient reported for adsorption from the gas phase.³⁸ The rate constant has been demonstrated to be sensitive to both the solvent and the alkane chain length.^{36,39,43} It was suggested that the rate-limiting step for the Langmuir uptake might involve the displacement of the solvent molecules by adsorbate molecules at the interface.^{27,38} In many reports, there is a second much slower uptake that results in the formation of the final, well-ordered film. In situ kinetic AFM studies suggest the presence of at least two phases during solution deposition: a "short" phase, attributed to the molecules lying in the surface plane, and an erect phase.⁴¹ In situ STM studies have reported two striped phases for decanethiol adsorption and one for octadecanethiol.⁴⁸

The spectra of the complete films presented in Figure 3 are consistent with the well-ordered final crystalline phase formed by both long-chain thiols and disulfides.^{18,19} In ordered monolayers where the hydrocarbon chains pack together tightly in an all-trans configuration, selection rules in the electric dipole approximation make methylene vibrational transitions SFG inactive.²⁹ Spectra of highly ordered monolayers are dominated by the symmetry-allowed CD_3 stretching modes from the terminal methyl group. The predominant features in Figure 3 are those of the terminal methyl. The feature assigned to d^+ at 2103 cm^{-1} is more prominent than the methylene features in published crystalline ODT films.^{25,49} The strength and relatively narrow line width of this feature are reproduced in numerous spectra formed from dODDS and dODT. This may reflect the quality of the Au substrates, or it may be indicative of slightly different relative hyperpolarizabilities between the protonated and deuterated methyl and methylene groups. IRAS studies of the structure of thiolate monolayers incubated over multiple days indicate that there is a slow orientational ordering of the chains.²³ The time constant of the final ordering step differs widely in the literature, ranging from hours to days.^{25,26} The similarity of the spectra in Figure 3 indicates that this final orientational ordering, reflected in the decrease in d^+ intensity and the slight increase in methyl intensity, is a small effect, that is, the film is nearly completely ordered after 14 min. This is in agreement with ex situ IRAS studies of docosanethiolate (C_{22}) monolayers,²⁶ in which well-ordered films were formed quickly from $5\text{ }\mu\text{mol/L}$ solutions, but in stark contrast with ex situ SFG studies of C_{22} at similar concentrations, in which well-ordered methyl features did not appear until well after nominal saturation of the thiolate coverage.²⁵

The SFG spectra at low coverages/early times clearly reflect a very different molecular structure. Most notable is the relative strength of the d^+ methylene intensity. The dominance of methylene stretches at early times indicates a high degree of gauche conformations in the hydrocarbon

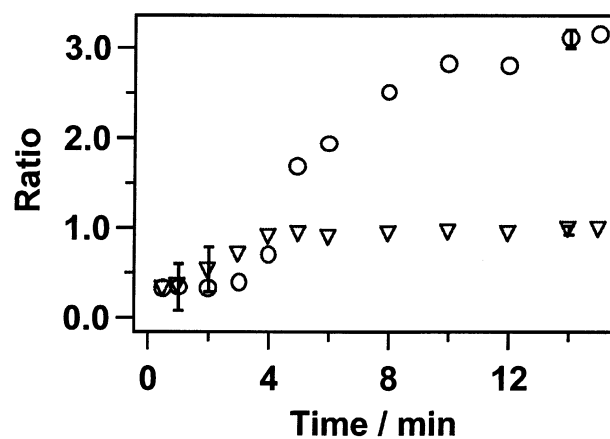


Figure 4. The evolution of ratios (○) of intensities of CD_3 and CD_2 symmetric stretches, A_{r^+}/A_{d^+} , and ratios (▽) of intensities of CD_3 asymmetric and CD_3 symmetric stretches, A_{r^-}/A_{r^+} .

chains of adsorbed molecules.^{50,51} Therefore, comparing the intensities of CD_3 and CD_2 symmetric bonds can yield information on the order of the alkyl chain within the thiolate monolayer. The evolution of the ratio of the intensities (A_i in eq 1) of the r^+ and d^+ features is plotted in Figure 4. A clear growth of an ordered state ($CD_3/CD_2 > 1$) from a disordered state ($CD_3/CD_2 < 1$) is observed. Additional insight into the low-coverage structure can be obtained from consideration of the ratio of the intensities of the r^+ and r^- features (also plotted in Figure 4). This intensity ratio can be related to the tilt angle of the methyl group from the surface normal. In the copropagating configuration used in our measurements, only the zzz and xxz elements of the susceptibility are expected to contribute significantly to the spectrum. Assuming local C_{3v} symmetry for the methyl group and averaging over methyl internal rotations, the r^- intensity will vanish for a methyl tilt angle of zero with respect to the surface normal.^{52,53} As the tilt angle increases, the r^-/r^+ ratio will increase. At a 90° tilt, the intensity of both modes will vanish, but the limiting r^-/r^+ ratio will be a maximum. The observation of approximately equal intensities for the two lines in the crystalline film structure corresponds to the majority of the methyl groups oriented at a tilt of $\sim 26^\circ$ based on IRAS studies of ODT films.²² The r^-/r^+ ratio decreases at low coverage, indicating that the C_{3v} axis of the methyl groups is oriented closer to the surface normal at low coverages than in the crystalline state, for example, $\sim 10\text{--}15^\circ$ rather than $\sim 26^\circ$.

The low-coverage spectra are not consistent with the alkane chain lying in the surface plane. The extended chain structure attributed to the striped phases would produce weak methylene features, unless the surface lowers the symmetry of the CD_2 groups. The development of "softened modes" in the spectra of hydrocarbons on surfaces due to symmetry lowering has been reported for a number of linear and cyclic alkanes.^{54,55} The modes were attributed to the CH stretching vibration in the vicinity of the metal surface, that is, the hydrocarbon chain contacting the substrate surface. No significant softened

(50) Walker, R. A.; Conboy, J. C.; Richmond, G. L. *Langmuir* **1997**, *13*, 3070.

(51) Smiley, B. L.; Richmond, G. L. *J. Phys. Chem. B* **1999**, *103*, 653.

(52) Lobau, J.; Wolfrum, K. *J. Opt. Soc. Am. B* **1997**, *14*, 2505.

(53) Bell, G. R.; Bain, C. D.; Ward, R. N. *J. Chem. Soc., Faraday Trans.* **1996**, *92*, 515.

(54) Manner, W. L.; Bishop, A. R.; Girolami, G. S.; Nuzzo, R. G. *J. Phys. Chem. B* **1998**, *102*, 8816 and references therein.

(55) Yamamoto, M.; Sakurai, Y.; Hosoi, Y.; Ishii, H.; Ito, E.; Kajikawa, K.; Ouchi, Y.; Seki, K. *Surf. Sci.* **1999**, *427/428*, 388.

(48) Yamada, R.; Uosaki, K. *Langmuir* **1998**, *14*, 855.

(49) Hines, M. A.; Todd, J. A.; Guyot-Sionnest, P. *Langmuir* **1995**, *11*, 493.

modes were observed, either in situ or ex situ, during this study for the adsorption of dODT or dODDS. This is in contrast with a recent ex situ SFG study of the adsorption of docosanethiol on gold,²⁵ where a strong and broad softened mode feature was continuously observed up to 0.6 monolayer coverage at a frequency of 2813 cm⁻¹. The frequencies and narrow widths we observe in the early-time spectra for the methylene modes are consistent with an upright (not lying in the surface plane) molecule with significant gauche disorder in the methylene chain. This orientation is consistent with the intermediate phase (liquid upright, not striped but not crystalline) observed by scanning tunneling microscopy (STM) for alkanethiol adsorption.

In the in situ STM experiments of Yamada and Uosaki,⁴⁸ striped phases were observed for the adsorption of decanethiol, pentadecanethiol, and octadecanethiol from heptane. The STM experiments were done with very dilute solutions so that adsorption was self-limiting to less than a monolayer. At higher concentrations, the striped phases were not observed, either because the transition from the striped phase to the intermediate phase (imaged as islands with no molecular structure) was too fast to be observed by STM or because the striped phase did not kinetically compete with direct formation of the intermediate phase. The absence of in situ spectroscopic evidence for the formation of striped phases in our study of dODDS may similarly be attributed either to a lack of sensitivity or to a failure of the striped phase to kinetically compete with the formation of the intermediate, disordered chain phase. A striped phase has recently been reported in ex situ STM studies of the adsorption of dODDS.⁵⁶

On the basis of the strong evidence for multiple phase coexistence following the adsorption of thiol molecules, we have tried to fit our SFG data for the adsorption of a disulfide with a simple two-phase model. We assume that the earliest time spectrum ($t = 0.5$ min) is the spectrum of surface species in phase I (disordered) and that the latest time spectrum ($t = 14$ min) is the spectrum of surface species in phase II (2D crystal). The spectra between these two states can be expressed as linear combinations of them:

$$\text{signal}(t) = |B(t) + \theta_I(t) \sum_{i=1}^7 \frac{A_i^I e^{i\phi_i^I}}{\nu_i^I - \nu_i^I + i\Gamma_i^I} + \theta_{II}(t) \sum_{i=1}^7 \frac{A_i^{II} e^{i\phi_i^{II}}}{\nu_i^{II} - \nu_i^{II} + i\Gamma_i^{II}}|^2 \quad (3)$$

in which θ_I and θ_{II} are the normalized coverages of surface species in phases I and II, respectively. In Figure 5, the SFG spectra of dODDS from Figure 1 are all refit by eq 3 with B , $\theta_I(t)$, and $\theta_{II}(t)$ as the only fitting parameters. $\theta_{II}(t=14 \text{ min}) \equiv 1$ while $\theta_I(t=0.5 \text{ min})$ was determined by $B(t=0.5 \text{ min})$. This simple two-phase model fits the data well. The fit parameters θ_I and θ_{II} are plotted in Figure 6 along with the total normalized coverage, θ_t , calculated from the nonresonant background B . An incubation time for θ_{II} is observed, and it indicates that the crystalline structure does not start to form until a certain critical time. A two-phase model is the simplest that can possibly explain the data. It is presumably too simple to be literally true; however, the model proves accurate enough to adequately explain the data.

We propose a simple phase equilibrium model to describe the evolution of the surface coverage. This model makes two assumptions about the self-assembly process: (i) at early times, the surface is covered with molecules in the disordered (liquid) phase with variable average density; and (ii) when the disordered phase density reaches a critical level, ρ_c (at $t = t_c$), the adsorbates segregate into regions of liquid (I) and solid (II) phases in coexistence, such that the total surface coverage is the sum of the surface coverage of these two phases. Adsorption in the disordered phase follows Langmuir kinetics, and direct adsorption into solid areas is forbidden. This model may be described by the following rate equations: for $t \leq t_c$,

$$\theta_t = \theta_I \quad (4a)$$

$$d\theta_t/dt = 2k_e C(1 - \theta_I) \quad (4b)$$

$$\theta_I = \rho_I S_I \quad (4c)$$

The normalized coverage, θ_I , is proportional to the number of the adsorbed molecules in phase I, which is equal to surface density of phase I, ρ_I (ρ_I is normalized to the saturation density of the solid phase, σ_{sat}), multiplied by the fractional surface area covered by phase I species, S_I . For $t < t_c$, S_I is equal to the total area S_t which is taken to be 1. θ_t is the total normalized thiolate coverage, and C is the concentration of disulfide in solution. k_e represents the effective Langmuir rate constant for total thiolate adsorption. For $t > t_c$,

$$\theta_t = \theta_I + \theta_{II} \quad (4d)$$

$$S_t = 1 = S_I + S_{II} \quad (4e)$$

$$\theta_I = \rho_c S_I \quad (4f)$$

$$\theta_{II} = \rho_{II} S_{II} = S_{II} \quad (4g)$$

$$d\theta_t/dt = 2k_e C(1 - \rho_c) S_I \quad (4h)$$

The normalized coverage θ_{II} is proportional to the number of the adsorbed molecules in phase II which is equal to the normalized surface density of phase II, $\rho_{II} \equiv 1$, multiplied by the surface area covered by phase II species, S_{II} . Equation 4h reflects that molecules stick only on the disordered phase. This equation can be shown to be equal to $d\theta_t/dt = 2k_e C(1 - \theta_t)$. Note that for $t > t_c$, ρ_I is constant (the fitted value described below = 0.49), while S_I decreases as adsorbing molecules increase the area of the crystalline phase at the expense of the area of the liquid phase. The corresponding integrated forms are

$$\theta_t = 1 - \exp(-2k_e C t) \quad (5a)$$

$$\theta_{II} = 0 \quad t \leq t_c$$

$$\theta_{II} = 1 - \exp(-2k_e C(t - t_c)) \quad t > t_c \quad (5b)$$

$$\theta_I = \theta_t - \theta_{II} = 1 - \exp(-2k_e C t) \quad t \leq t_c$$

$$\theta_I = \theta_c \exp(-2k_e C(t - t_c)) \quad t > t_c \quad (5c)$$

$$\theta_c = 1 - \exp(-2k_e C t_c) \quad (5d)$$

We used eqs 5a–d to fit the coverage versus time data of both phases and found good agreement between the data and the prediction of the simple model represented by the solid lines in Figure 6. The sharp cusp in θ_I as predicted

(56) Noh, J.; Murase, T.; Kakajima, K.; Lee, H.; Hara, M. *J. Phys. Chem. B* **2000**, *104*, 7411.

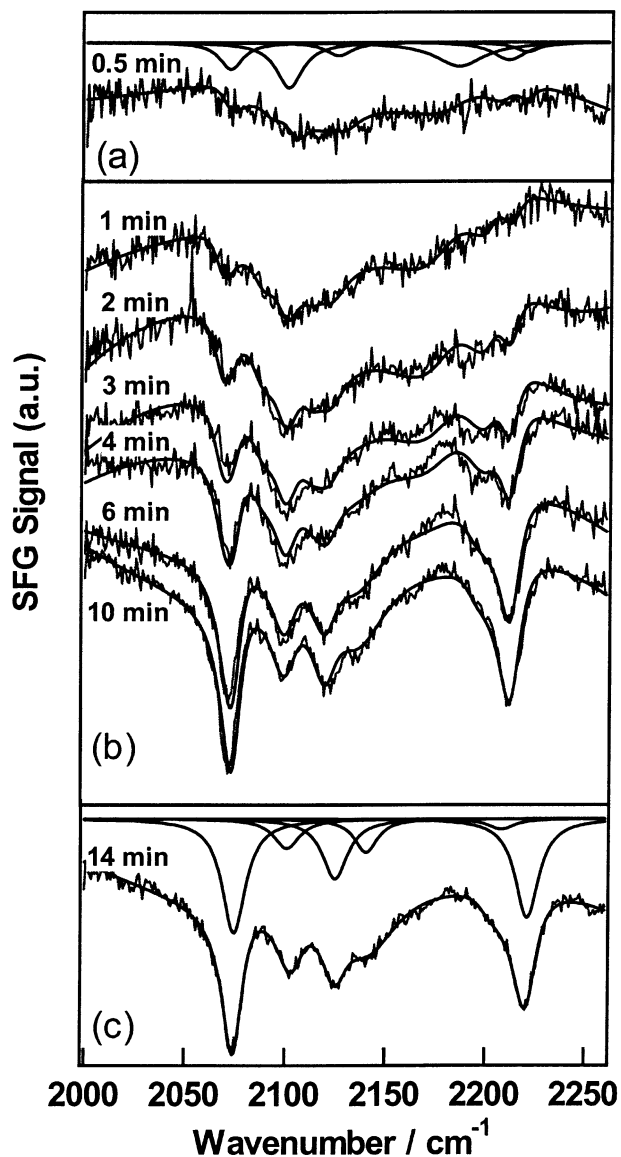


Figure 5. SFG spectra fit to the two-phase model: (a) shows the experimental SFG spectrum at $t = 0.5$ min and the fit to eq 3 assuming $\theta_{II} = 0$ (also shown are the imaginary parts of the fit representing phase I); (c) shows the experimental SFG spectrum at $t = 14$ min, and the fit to eq 3 assuming $\theta_I = 0$, representing phase II; (b) shows the SFG spectra at intermediate times fit to eq 3 with varying contributions from θ_I and θ_{II} .

by eq 5c is smoothed in the data, possibly due to inhomogeneities in the film averaged over the sample area probed by the laser beams. We also fit data acquired under different flow and concentration conditions. Table 3 summarizes all the fitted parameters including rate constants and critical coverage (θ_c). The model well describes all three sets of conditions. The rate constants, k_e , for total thiolate adsorption are found to be identical to the rate constant k acquired by simple Langmuir fitting of the nonresonant background B . The critical normalized coverage $\rho_I = 0.49 \pm 0.07$ is very similar to the maximum normalized coverage of the intermediate phase observed in ultrahigh vacuum, prior to development of crystalline islands for decanethiol.⁴⁶ The maximum stripe phase coverage would be expected to be ~ 0.2 .⁴⁸

This model is very similar to one proposed by Xu et al. to describe their in situ atomic force microscopy (AFM) data for the adsorption of thiol;⁴¹ except for scale factors, their Figure 9 is extremely similar to our Figure 6.

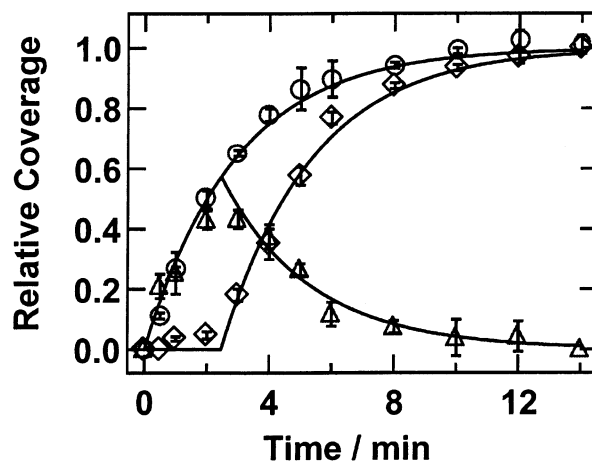


Figure 6. Total coverage, θ_t (○), converted from the nonresonant background B using $B = B_0 - R\theta_t$, as a function of surface exposure time. θ_I (△) and θ_{II} (◇) are the coverages of surface species I and II; $\theta_t = \theta_I + \theta_{II}$. The solid lines represent the fits to the phase equilibrium model (eq 5). The error bars represent the differences between two independent measurements.

Table 3. Rate Constants and Incubation Times from the Two-Phase Model^a

	dODDS concentration ($\mu\text{mol L}^{-1}$)		
	0.24	0.48	0.24
flow rate (mL/min)	0.68	0.68	1.1
k_e ($\times 10^4 \text{ L s}^{-1} \text{ mol}^{-1}$)	1.2 ± 0.03	0.89 ± 0.02	1.0 ± 0.03
t_c (min)	2.1 ± 0.11	1.6 ± 0.05	2.3 ± 0.12
corresponding relative coverage	0.51 ± 0.10	0.54 ± 0.05	0.49 ± 0.07

^a The errors are calculated from the fits of eq 5 to the data.

However, Xu et al. attributed phase I to physisorbed species lying down on the Au surface. Physisorbed species are not expected to produce a significant change in the nonresonant background in the SFG experiment and thus do not account for the observed Langmuir kinetics for thiolate formation in our experiments. In the model of ref 41, a phase I molecule occupies 4 times the area of an upright chemisorbed phase II molecule, so the I to II phase transition exposes the Au substrate. It was assumed that adsorption into the exposed regions was fast compared to the phase transition. However, evaluation of the rate constants in the model of Xu et al. indicates that the rate for the phase I to phase II transition is the same as the rate for adsorption into phase I.⁴¹ Thus, adsorption into phase I may be rate limiting, and the phase transition behavior may be nearly in equilibrium.

It is somewhat surprising that a simple Langmuir model (see Figure 2) effectively describes thiolate chemisorption, given the varied surface structures present and particularly in light of the strong coverage dependence of the sticking coefficient observed in vapor deposition.⁴⁶ The simple two-phase equilibrium model naturally accounts for the observation of Langmuir kinetics above the critical coverage, as the microenvironment of the disordered regions does not change with increasing coverage (until very near saturation). At first glance, the assumption of Langmuir kinetics, that is, negligible interactions between adsorption sites, would seem to not apply except at very low coverage (for adsorption below θ_c). One would expect that molecules already adsorbed would affect the approach of additional molecules to the surface, causing deviation from the Langmuir curve for thiolate formation as θ_t approaches θ_c . However, if the displacement of solvent molecules from the surface region is the rate-limiting step of adsorption,^{27,38} hindering of the approach of an adsorbing

molecule to the surface by the adjacent thiolate molecules would not be rate limiting.

V. Summary

In situ, vibrationally resonant sum frequency generation studies of the assembly of perdeuterated dioctadecyl disulfide on vapor-deposited Au substrates reveal that the structure of adsorbed thiolate fragments varies with coverage. At low coverage, the adsorbates are extended from the surface, highly disordered with significant gauche defects in the backbone but with a near-normal orientation for the terminal methyl group. At high coverage, the structure changes to the well-characterized, erect, tilted,

all-trans configuration characteristic of the crystalline full monolayer. The coverage evolution of the SFG spectra can be well described by the coexistence of two distinct phases: a low-coverage, disordered phase and the full-coverage crystalline phase. The kinetics of the evolution of these two phases can be quantitatively described by a simple model evoking phase coexistence above a critical density of the disordered phase.

Acknowledgment. Clayton Yang is a NIST National Research Council postdoctoral research associate.

LA0257790